

NANoREG

Grant Agreement Number 310584

Deliverable D 4.10

Particle distribution of MNM in hepatic and liver cell models

Due date of deliverable: 2016/02/28

Actual submission date: 2016/06/30

Author(s) and company:	Jungnickel, Harald, Tentschert, Jutta, Laux, Peter (all BfR), Fessard, Valerie (ANSES)
Work package/task:	WP4 / Task 4.5.4.1
Document status:	draft / <u>final</u>
Confidentiality:	confidential / restricted / <u>public</u>
Key words:	

DOCUMENT HISTORY

Version	Date	Reason of change
1	2016/06/24	Completion of the document
2	2016/08/31	Final updates
3	2017/02/21	Project Office harmonized lay-out
4		

This work is licensed under the Creative Commons Attribution-NonCommercial-ShareAlike 4.0 International License.

To view a copy of this license, visit <http://creativecommons.org/licenses/by-nc-sa/4.0/> or send a letter to Creative Commons, PO Box 1866, Mountain View, CA 94042, USA.

*This project has received funding from the European Union
Seventh Framework Programme (FP7/2007-2013)
under grant agreement no 310584*



ad beneficiary for this deliverable:

Owner(s) of this document	
Owner of the content	BfR, partner no. 6, ANSES, partner no. 35

Table of Content

1	DESCRIPTION OF TASK	4
2	DESCRIPTION OF WORK & MAIN ACHIEVEMENTS	4
2.1	SUMMARY	4
2.2	BACKGROUND OF THE TASK	4
2.3	DESCRIPTION OF THE WORK CARRIED OUT	4
2.3.1	Nanomaterials	4
2.3.2	Culture of Caco2 cells	4
2.3.3	Transmission electronic microscopy (TEM)	5
2.3.4	Investigations by Time-of-Flight secondary mass spectrometry (ToF-SIMS)	5
2.3.5	Cytotoxicity	6
2.3.6	HCS content analysis of active caspase 3 and phosphorylation of H2AX	6
2.4	RESULTS	6
2.4.1	Uptake	6
2.4.1.1	TEM	6
2.4.1.2	ToF-SIMS	9
2.4.2	Toxicity	15
2.4.2.1	Cytotoxicity	15
2.4.2.2	Interleukin 8 release	16
2.4.2.3	Markers of toxicity by HCS	16
2.4.2.4	Supplementary data: Genotoxicity	17
2.5	EVALUATION AND CONCLUSIONS	17
2.6	DATA MANAGEMENT	17
3	DEVIATIONS FROM THE WORK PLAN	17
4	PERFORMANCE OF THE PARTNERS	ERROR! BOOKMARK NOT DEFINED.
5	REFERENCES / SELECTED SOURCES OF INFORMATION (OPTIONAL)	18
6	LIST OF ABBREVIATIONS (OPTIONAL)	18
	ANNEXES (OPTIONAL)	18

1 Description of task

Pattern of particle distribution *in vitro* and *in vivo*

The aim is to assess the relevance of systemic genotoxicity and particle distribution of MNM. Preparation of up to 50 samples from *in vitro* and *in vivo* systems for structural analysis by ToF-SIMS. These structural investigations will relate particle occurrence and distribution to the studies on genotoxicity in Task 4.5.4.

2 Description of work & main achievements

2.1 Summary

HepaRG cells were shown in a 3D reconstruction to internalize nanoparticles following exposition against 47.5 mg/ml of TiO₂ NM-104. The compound was detected in the form of agglomerates with a size range between 1 and 20 µm. In association with these agglomerates, an enhanced abundance of aluminium was detected.

2.2 Background of the task

TiO₂ in its anatase form as well as in anatase-rutile mixtures was found to induce DNA-damage in several cell types as e.g. keratinocytes or colon epithelial cells *in vitro*. At the same time, *in vivo* assays have generated almost no genotoxic effects. Beside inflammation-mediated secondary genotoxicity, generation of oxidative stress is currently discussed as a mechanism of potential genotoxic effects of TiO₂. For chemicals in general, cellular distribution and internalization is considered a major factor for genotoxicity. As the intestinal epithelium represents a major barrier for TiO₂ following ingestion, we investigated internalization of TiO₂ by Caco2 intestinal cells employing time-of-flight secondary ion mass spectrometry (ToF-SIMS). It is important to evaluate in which cell compartments the NPs are detected as well as in which form they are encountered as these parameters may have an impact on the behaviour of the NPs over time and the effects expected at the cellular level.

This task may interlink with other tasks such as WP5.3, WP5.5 and WP5.6 as results on Caco2 cells with TiO₂ are expected within these tasks.

2.3 Description of the work carried out

The NANoREG core material NM103 was investigated and compared to NM104, a material of similar composition and size but without a hydrophobic surface.

First, the uptake and distribution inside the differentiated human intestinal Caco2 cells were analysed after an acute (24h) exposure. In a second step, the behaviour of NPs was measured after repeated exposure as well as after a period of recovery.

2.3.1 Nanomaterials

The study was performed on two rutile forms of TiO₂ sharing similar size and composition but possessing a different coating: NM 103 and NM104. The nanoparticles were dispersed according to the NANoREG [Guidance Document](#).

2.3.2 Culture of Caco2 cells

Acute exposure (24h) for ToF SIMS

For ToF-SIMS analysis, cells were cultivated on wafers (polished size up) in 24 wells plates. Caco2 cells were seeded at a density of 20 000 cells/cm². Culture medium was changed three times a week. Cells were differentiated during 25–27 days post-seeding. NPs (NM103 and NM104 provided by the JRC) were dispersed in a mixture of water/BSA 0.05 % (p/v) according to the NANoREG Guidance Document. Differentiated Caco2 were incubated with 3 concentrations of each NP (0.75, 3.13 and 12.5 µg/cm²) (2 replicates per concentration) for 24h.

After exposure the cells were rinsed twice with NH_4CO_3 (144 mM), collected gently, fast-frozen in liquid nitrogen and freeze-dried for the ToF-SIMS analysis.

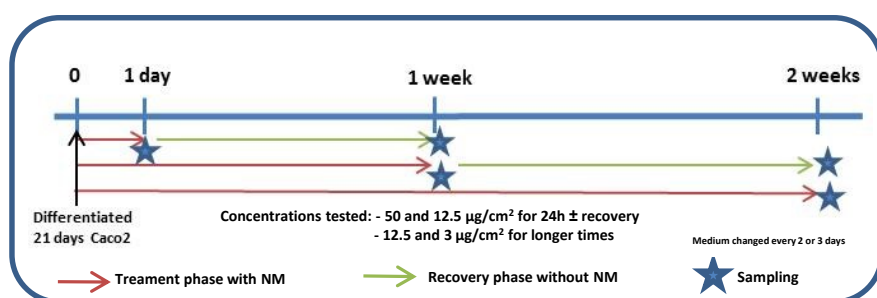
Repeated exposure with or without a recovery period

Cells were seeded at 20.000 cells/cm². Culture medium was changed three times a week. Cells were differentiated during 21 days post-seeding.

Cells were repeatedly exposed to NM103 or NM104: medium was changed every two or three days and replaced by new medium supplemented with fresh NP solution prepared according to the NANoREG Guidance Document. Cells were exposed for 1 day, 1 week or 2 weeks. In some cases, exposure was followed by a recovery period of up to 1 week as described below. The concentrations were:

From 6.5 to 50 $\mu\text{g}/\text{cm}^2$ for 24h exposure

From 3 to 12.5 $\mu\text{g}/\text{cm}^2$ for 1 and 2 weeks exposure.



Treatment schedule for acute and repeated exposure of differentiated Caco2 cells to NM103 and NM104 followed or not by a recovery period (up to 1 week). After exposure, the cells were harvested for estimation of cytotoxicity (Neutral Red Uptake) and IL8 release. Immunostaining of toxicity markers linked with a TEM detection was performed for High Content Screening.

2.3.3 Transmission electronic microscopy (TEM)

Caco-2 cells were seeded in 35 mm Petri dishes at a density of 20.000 cells/cm². After differentiation, cells were exposed to NM103 and NM104 in a concentration of up to 256 $\mu\text{g}/\text{ml}$ for 24 h. After rinsing twice with PBS and with 0.15 M Na cacodylate buffer, cells were fixed by drop wise addition of glutaraldehyde (2.5 %) for 1 h and analysed according to conventional methods. The cells were rinsed several times with 0.15 M Na cacodylate buffer and post fixed with 1.5% osmium tetroxide for 1 h. After further rinsing with cacodylate buffer, the samples were dehydrated through an ethanol gradient from 70 % to 100 % and infiltrated in a mixture of acetone-eponate (50/50) for 3 h and subsequently in pure eponate for 16 h. Finally, the samples were embedded in DMP30-Eponate for 24 h at 60 °C. Sections (0.5 μm) were cut with a LEICA UC7 microtome and stained with toluidine blue. Ultra-thin sections (90 nm) were collected onto copper grids and counterstained with 4 % uranyl acetate and subsequently with lead citrate (Reynold solution). Examination was performed with a JEOL 1400 electron microscope operated at 120 kV.

2.3.4 Investigations by Time-of-Flight secondary mass spectrometry (ToF-SIMS)

Time-of-flight secondary ion mass spectrometry (ToF-SIMS) in combination with argon cluster ion sputtering was used to investigate TiO_2 nanoparticle agglomerates within Caco2 cells. This cell line was originally acquired from a colon adenocarcinoma. The analysis of this material was scheduled to get insights into the TiO_2 particle/agglomerate distribution *in vivo* as well as in the occurrence of contaminants on single cell level. Depth profile and images taken as a function of depth were obtained using an Ar cluster ion beam for sputtering and Bi^{3+} primary ions for the analysis. The ToF-SIMS depth profiles were obtained by first analysing the surface with Bi^{3+} primary ions with an analysis area of 200 x 200 μm^2 . The same spot was sputtered with the Ar cluster ion beam using a raster area of 500 x 500 μm^2 . Again, analysis and sputtering were alternated out until 360 images were obtained at different depths. Analysis was performed using a 512 x

512 pixel raster. The data were evaluated using the Surface Lab software (ION-TOF GmbH, Münster, Germany).

2.3.5 Cytotoxicity

The Neutral Red Uptake (NRU) was performed in 96 well-plates on differentiated Caco2 cells. After treatment, the medium was removed and 100 µl of 0.003% NR solution were added to each well. After a 3-h incubation period, the NR solution was discarded and 100 µl of 1% acetic acid solution containing 50 % ethanol were added in order to extract the dye from the cells. The absorbance at 540 nm was then evaluated using a spectrophotometer (Fluostar Optima, BMG Labtech).

2.3.6 HCS content analysis of active caspase 3 and phosphorylation of H2AX

Rabbit anti-active caspase 3 (ab13847) primary antibodies were purchased from Abcam, and mouse anti phosphorylated H2AX primary antibodies, secondary anti-rabbit and anti-mouse antibodies were acquired from Thermofisher Scientific.

After treatment, cells were rinsed twice with PBS and fixed with 4 % formaldehyde. After permeabilization with 0.2 % PBS-Triton X100 for 10 min, cells were washed twice with 0.05 % PBS-Tween-20 and saturation was performed with 1% BSA in PBS-Tween-20 (0.05 %) for 30 min at room temperature. Cells were then incubated overnight with primary antibodies: rabbit anti-caspase 3 (1:1000) and mouse-anti phospho H2AX (γH2AX) (1:1500). After 3 washes with 0.05 % PBS Tween, cells were incubated for 45 min with the 2nd antibody (1:1000) (Ig G H+L) anti-rabbit conjugated with DyLight 488 or anti mouse conjugated with DyLight 550. After washing with 0.05 % PBS-Tween, nuclei were stained with DAPI (1 µg/ml).

Images were acquired with the Arrayscan VTi (Thermo Scientific/Cellomics) and were analysed using the Target Activation bioapplication. Four wells per condition and ten fields per well were analysed. The mean average fluorescence intensity corresponding to the mean of the average pixel intensity per object for each well.

2.4 Results

2.4.1 Uptake

2.4.1.1 TEM

After acute and repeated exposure, NM 103 and 104 were taken up by Caco2 cells (Figure 1) and accumulated over time inside the cells. Particles remained inside the cells even after a recovery period (Figure 2).

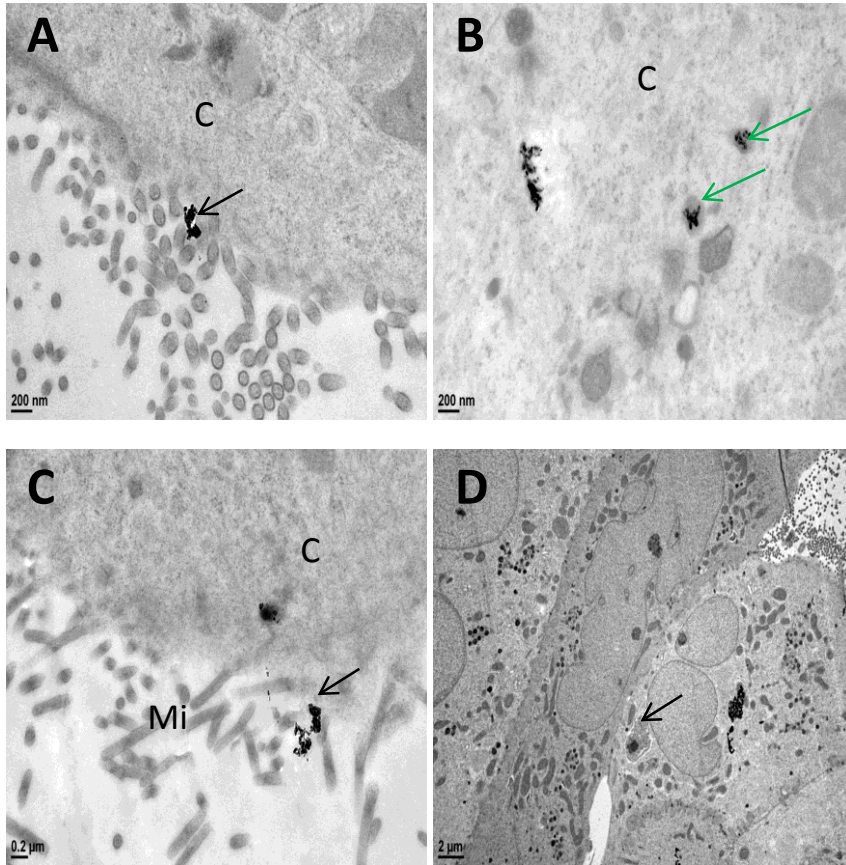


Figure 1: TEM images of differentiated Caco2 cross sections showing the uptake of NM103 (A,B) and NM104 (C,D) agglomerates in endosome-like vesicles (green arrow) by membrane invagination (black arrows). C: cytoplasm, Mi: microvilli.

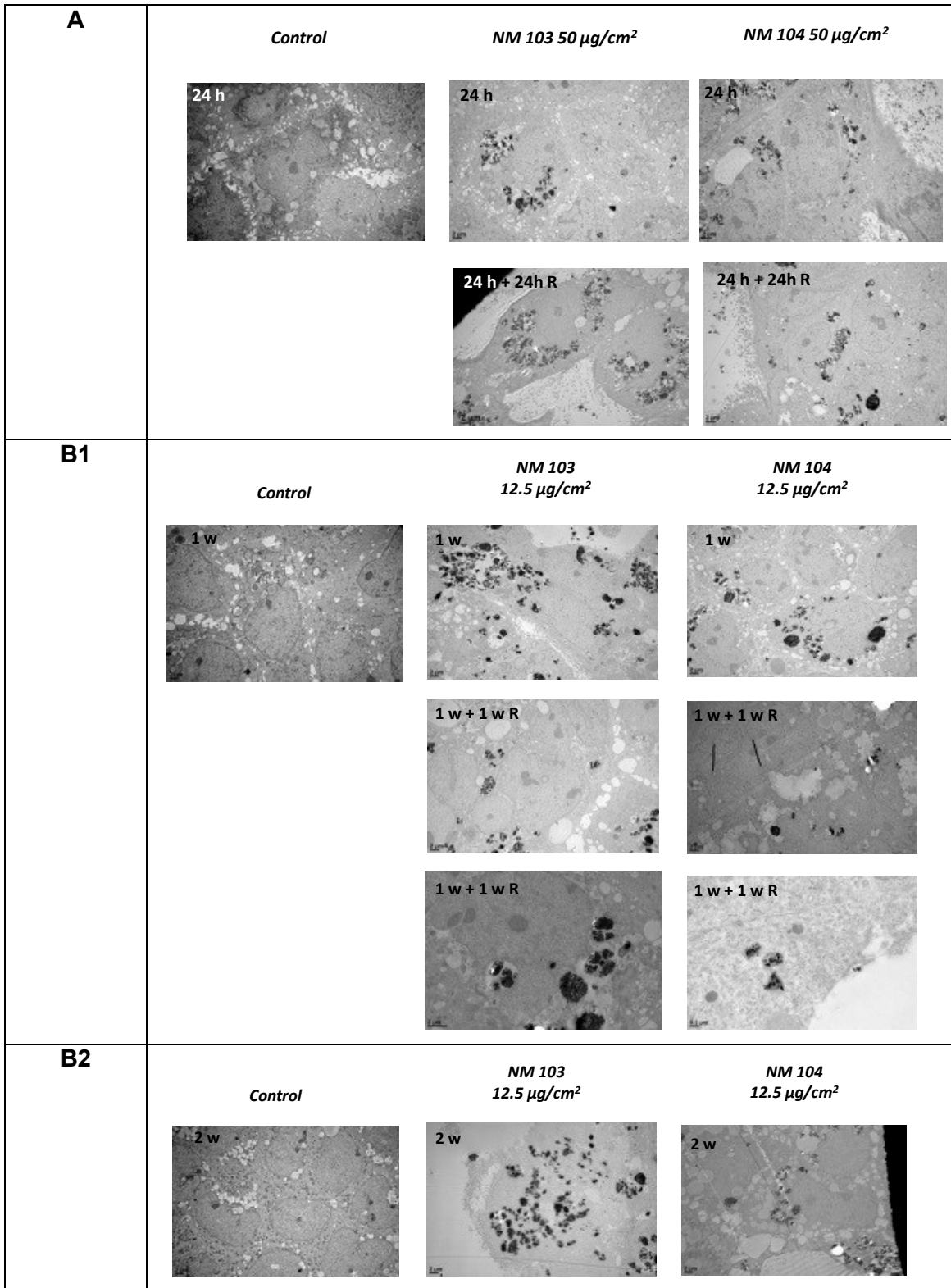


Figure 2: Uptake of NM103 and NM104 in differentiated Caco2 cells after: **A)** An acute treatment (24h) followed or not by one day recovery; **B)** A longer treatment followed or not by a recovery period (24h or 1 week): 1) after one week exposure and 2) after 2 weeks exposure

2.4.1.2 ToF-SIMS

The spectra for the depth profiles revealed a strong signal being present in TiO₂ exposed Caco2 cells in comparison to control cells for both nanoparticles tested, NM-103 and NM-104. (see Fig. 3).

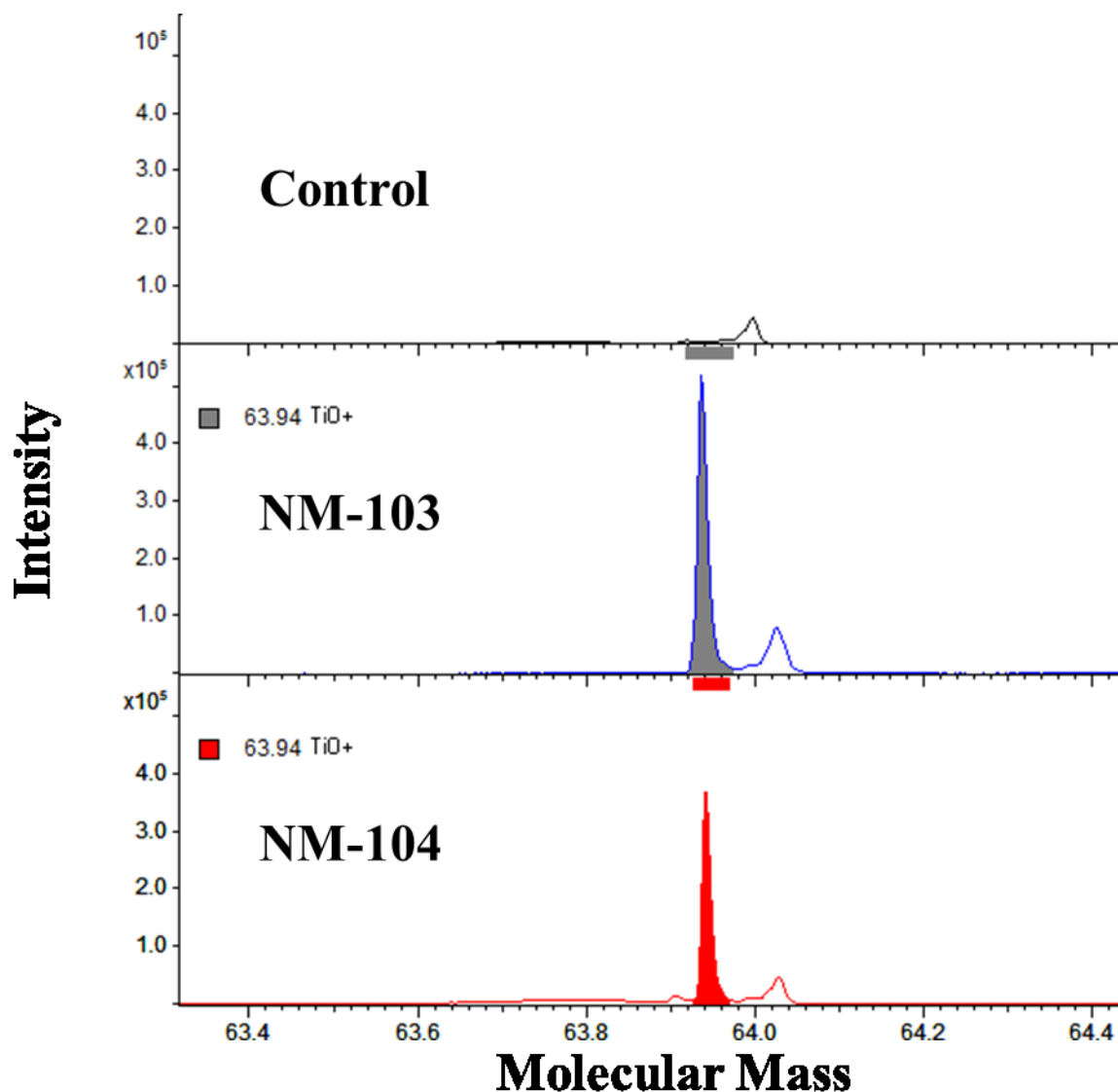


Figure 3: ToF-SIMS spectra, showing the TiO⁺ ion peak, derived from depth profiles of unexposed Caco-2 cells (control) and Caco-2 cells exposed against 12.5 $\mu\text{g}/\text{cm}^2$ of NM-103 or NM-104.

Further data analysis using a 3D reconstruction showed that single cells indeed had TiO₂ nanoparticle agglomerates incorporated (see Figures 4 and 5). The 3D reconstruction of the nanoparticle agglomerate within the single cell was used to reconstruct only the nanoparticle agglomerate (see Figures 5 and 6). Fig. 5 reveals a larger nanoparticle agglomerate (see I in Fig. 5) within a single cell, which is surrounded by smaller nanoparticle agglomerates (see II in Fig. 5).

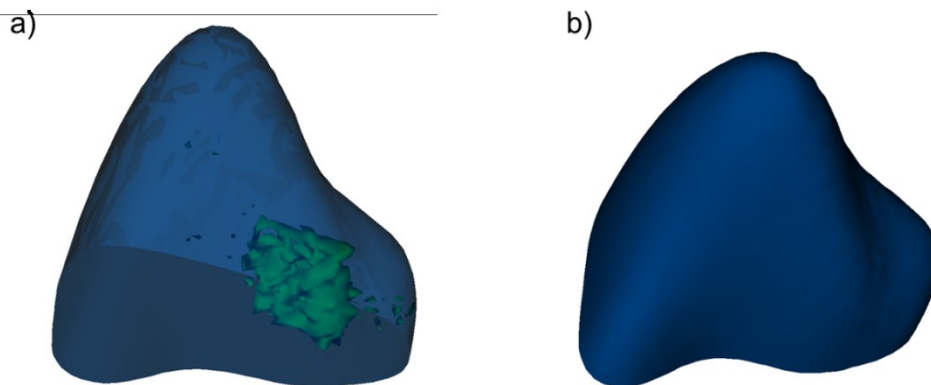


Figure 4: ToF-SIMS depth profile reconstruction of a Caco-2 cell, for 24h exposed to 12.5 $\mu\text{g}/\text{cm}^2$ TiO₂ NM-104, showing a single Caco-2 cell (ca. 40 μm x 8 μm), reconstructed from the C₃H₈N⁺ signal (blue, cell outline) and the TiO₂ nanoparticle agglomerates within the single cell, reconstructed from the TiO⁺ ion peak (depicted in green). a) shows the cell outline in transparent blue where the green nanoparticle agglomerates within the single cell are clearly visible. b) shows the blue cell outline in solid blue. No nanoparticle agglomerates are visible anymore, indicating nanoparticle uptake by Caco-2 cells.

The 3D reconstruction of the nanoparticle agglomerate within the single cell was used to investigate its structure in more detail (see Figure 5). Figure 5 reveals a large size central agglomerate (see I in Figure 5) within a single cell, which is surrounded by smaller ones (see II in Figure 5).

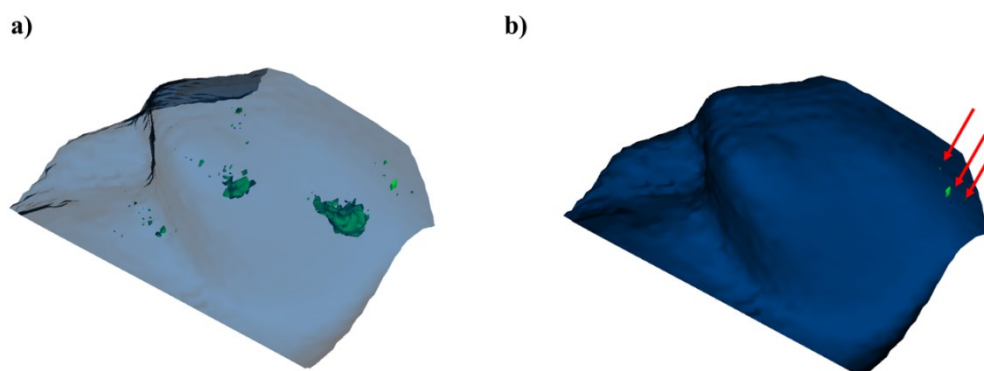


Figure 5: ToF-SIMS depth profile reconstruction of a Caco-2 cell, for 24h exposed to 12.5 $\mu\text{g}/\text{cm}^2$ TiO₂ NM-103, showing a single Caco-2 cell (ca 35 μm x 15 μm), reconstructed from the C₃H₈N⁺ signal (transparent blue cell outline) and the TiO₂ nanoparticle agglomerates within the single cell, reconstructed from the TiO⁺ ion peak (depicted in green). The red arrows depict three nanoparticle agglomerates, which seem to stick in the single cell, one part being visible on the outside, the other part sticking in the cell membrane and within the single cell.

ToF-SIMS 3D depth profile spectra from nanoparticle agglomerates were further used to identify impurities within nanoparticle agglomerates, localized within single cells.

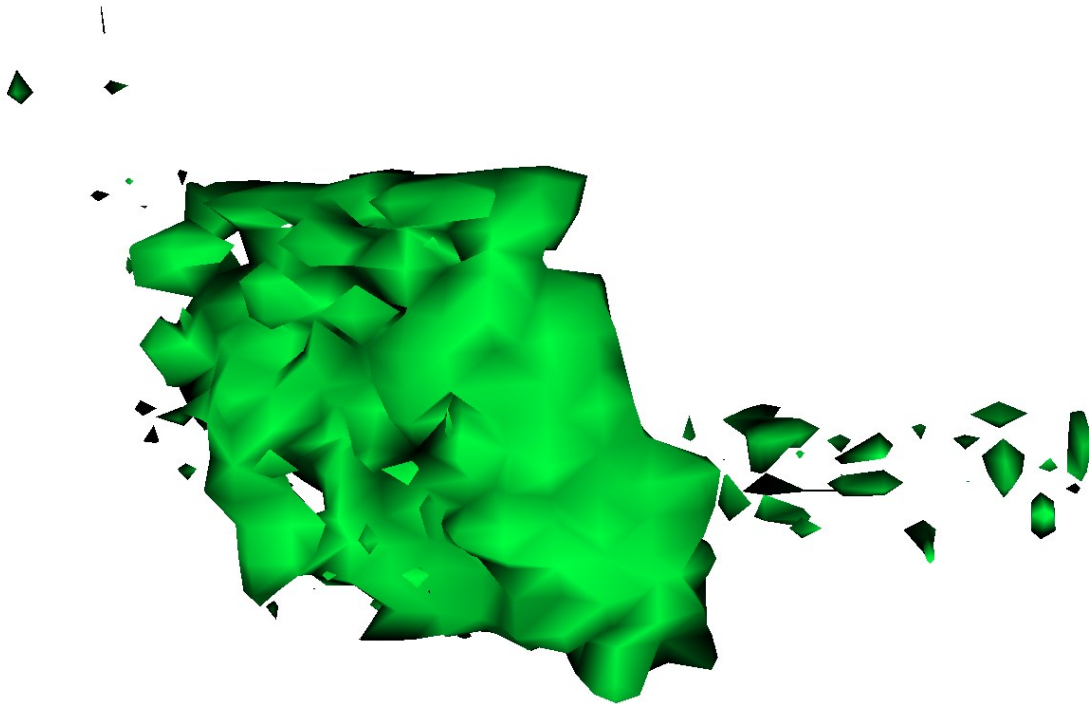


Figure 6: ToF-SIMS 3D depth profile reconstruction of TiO₂ NM-104 nanoparticle agglomerates within a single cell, reconstructed from the TiO⁺ ion peak (depicted in green). Clearly visible is one larger irregular shaped nanoparticle agglomerate accompanied by smaller irregular shaped nanoparticle agglomerates.



Figure 7: ToF-SIMS 3D depth profile reconstruction of TiO₂ NM-103 nanoparticle agglomerates within a single cell, reconstructed from the TiO⁺ ion peak (depicted in green). Clearly visible are three larger irregular shaped nanoparticle agglomerates accompanied by smaller irregular shaped nanoparticle agglomerates.

For a first insight into the TiO₂ particle distribution after exposure, one depth profile (300 μm x 300 μm) each was analysed for Caco-2 cells exposed to NM-103 or NM-104 TiO₂ nanoparticles at a dose of 12.5 μg/cm². The depth profiles revealed for both materials that not all single cells in the analysed area had taken up nanoparticle agglomerates. The TiO⁺ agglomerates from the acquired ToF-SIMS pictures were analysed for total agglomerate counting and agglomerate size determination using the freeware programme DotCount v1.2 (MIT freeware programme). All agglomerates were categorized into three groups: Group 1: 100 nm² agglomerate size, Group 2: 100 – 500 nm², Group 3: 500 – 1 μm², Group 4: 1 to 5 μm², Group 5: 5 to 10 μm², Group 6: 10 to 30 μm², Group 7: > 30 μm². An overview of the observed agglomerate numbers in NM-103 and NM-104 exposed Caco-2 cells is shown in Figures 8 and 9.

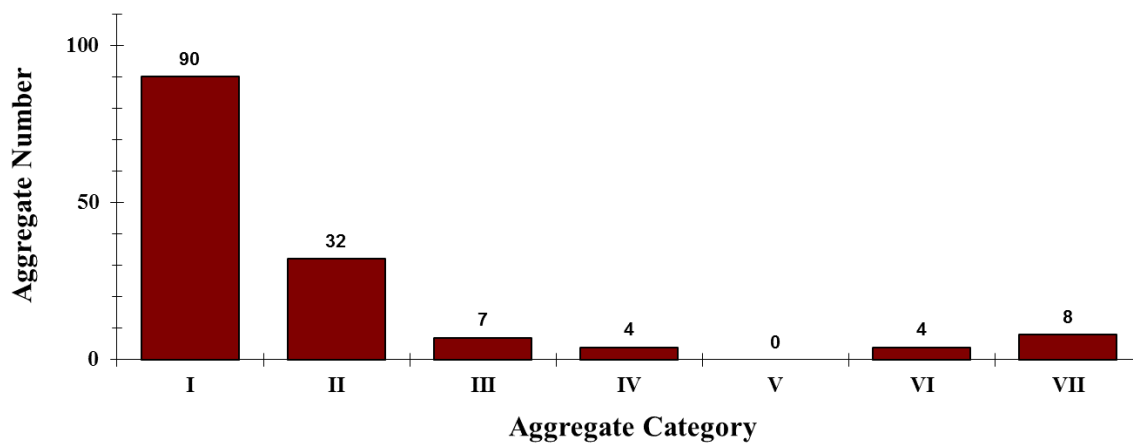


Figure 8: TiO₂ nanoparticle agglomerate categorization from a total area of 300 x 300 μm² of differentiated Caco-2 cells exposed to NM-103: Group 1: 100 nm² agglomerate size, Group 2: 100 – 500 nm², Group 3: 500 nm² – 1 μm², Group 4: 1 to 5 μm², Group 5: 5 to 10 μm², Group 6: 10 to 30 μm², Group 7: > 30 μm². Agglomerate counts are indicated as numbers above each column. Total number of agglomerates counted: 145.

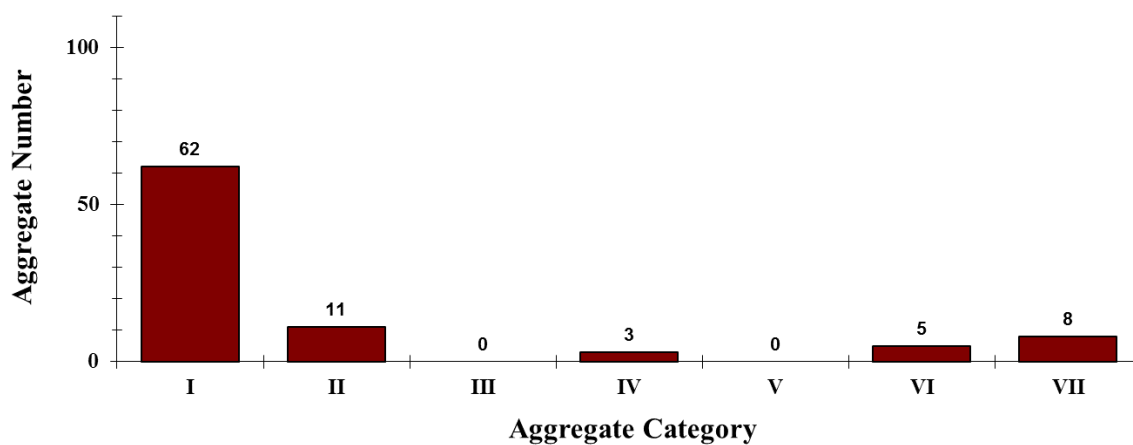


Figure 9: TiO₂ nanoparticle agglomerate categorization from a total area of 300 x 300 μm² of differentiated Caco-2 cells exposed to NM-104: Group 1: 100 nm² agglomerate size, Group 2: 100 – 500 nm², Group 3: 500 nm² – 1 μm², Group 4: 1 to 5 μm², Group 5: 5 to 10 μm², Group 6: 10 to 30 μm², Group 7: > 30 μm². Agglomerate counts are indicated as numbers above each column. Total number of agglomerates counted: 89.

For both TiO₂ nanoparticles, NM-103 and NM-104, the smallest agglomerate group, Group I: 100nm² is the fraction with the highest particle number in Caco-2 cells, followed by the next larger particle group, Group II: 100 to 500 nm² indicating a high number of smaller particle agglomerates in Caco-2 cells for both nanoparticles (NM-103 and NM-104).

ToF-SIMS 3D depth profile spectra from nanoparticle agglomerates were used to identify the distribution of $K_2SO_4H^+$ ions within nanoparticle agglomerates for both nanoparticles, NM-103 and NM-104, localized within single cells. An area of interest, comprising the nanoparticle agglomerate from a single cell only was used for the assessment.

To assess the distribution of the ion $K_2SO_4H^+$ within the nanoparticle agglomerate, the ratio of $K_2SO_4H^+/TiO^+$ ions was investigated within the 3D depth profile of a nanoparticle agglomerate. The results are shown in figures 10 and 11. For NM-103, figure 10 shows a higher amount of $K_2SO_4H^+$ ions in comparison to TiO^+ in the outer layers of the agglomerate until ca. 110 nm depth with the highest ratio being 2.5 in the outermost agglomerate layers. From 160 nm depth the ratio $K_2SO_4H^+/TiO^+$ is rather constant around 0.4. For NM-104 figure 9 reveals higher amounts of $K_2SO_4H^+$ in comparison to TiO^+ in the outer agglomerate layers until ca. 360 nm depth in comparison to only 110 nm for NM-103. Also NM-104 shows a much higher $K_2SO_4H^+/TiO^+$ ratio (10.6) than NM-103 (2.5) in the outermost agglomerate depth layers. For NM-104 from ca. 1 μm depth the ratio is rather constant with around 0.4.

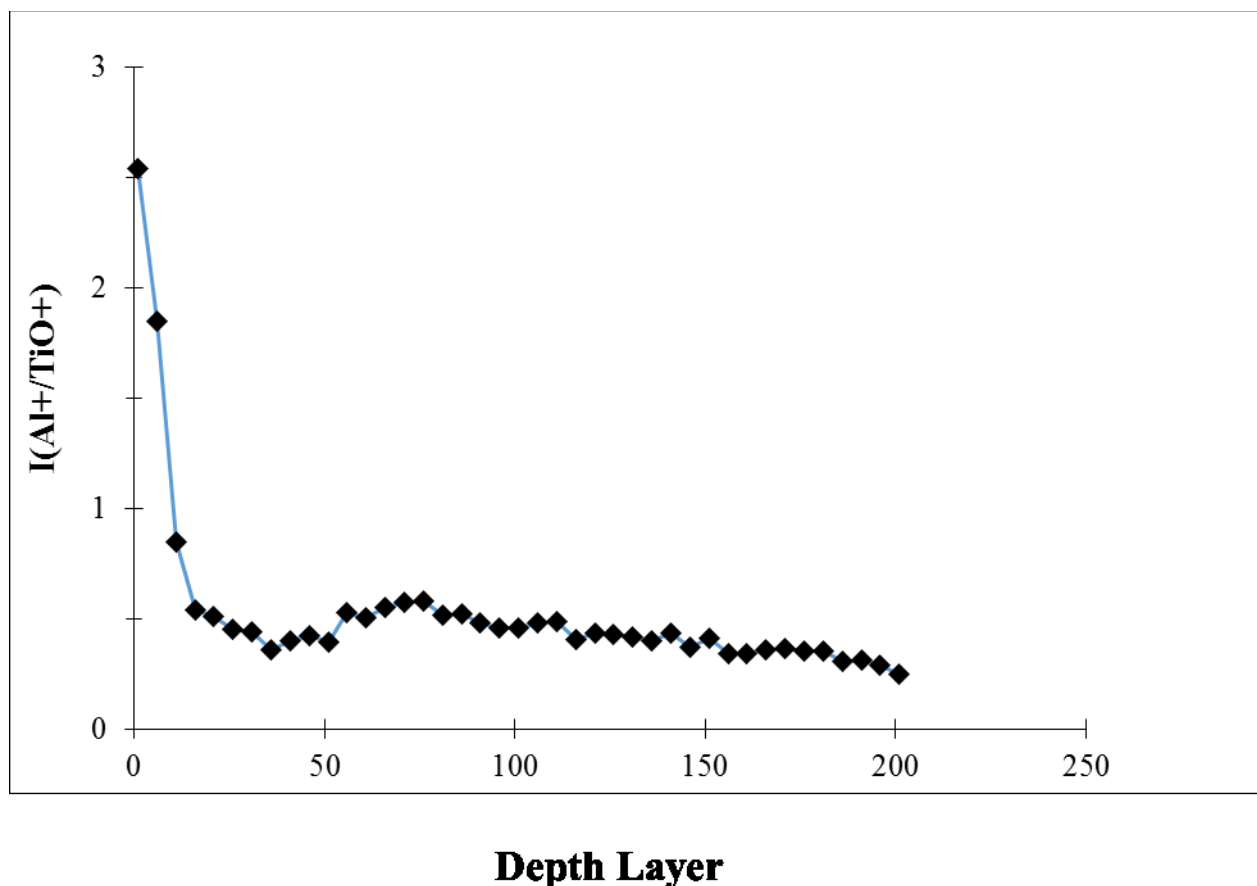


Figure 10: $K_2SO_4H^+/TiO^+$ ion ratio derived from depth profiles from one agglomerate, identified in a single Caco-2 cell exposed to $12.5 \mu g/cm^2$ of NM-103.

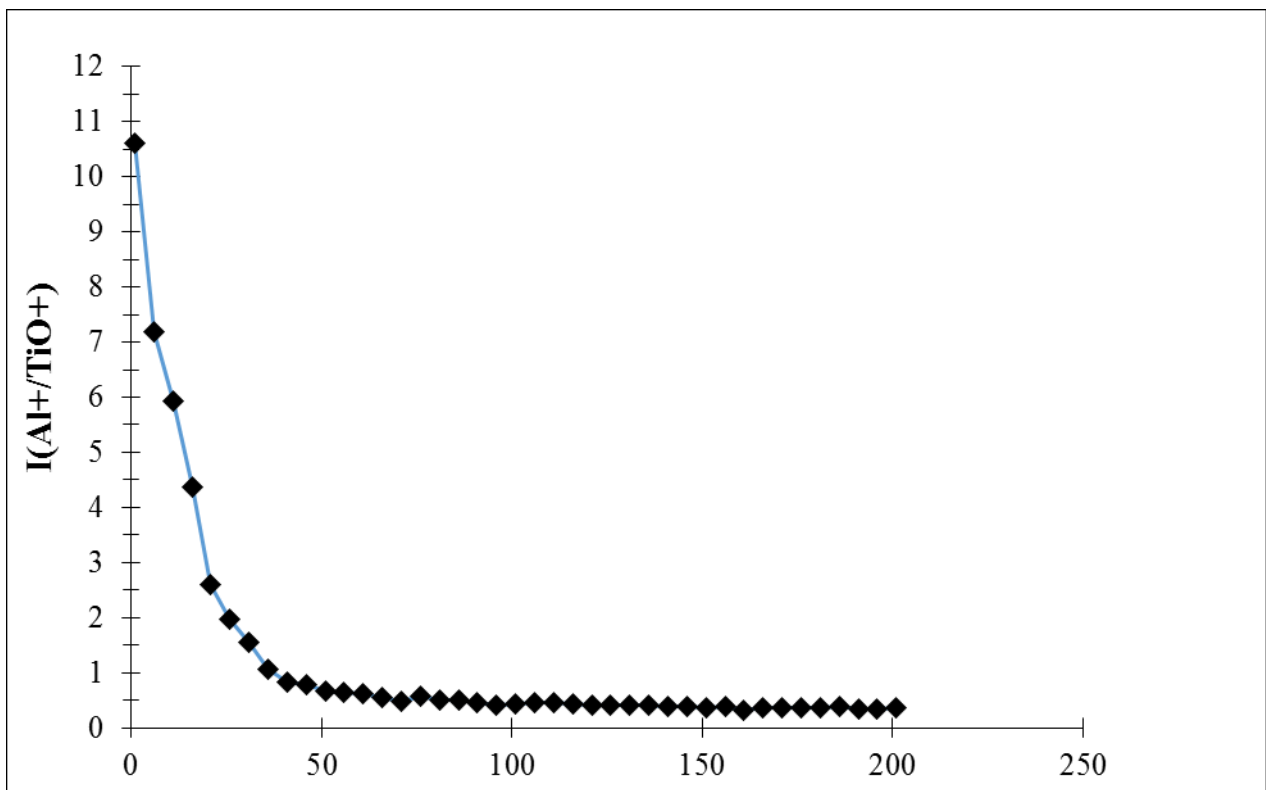


Figure 11: $\text{K}_2\text{SO}_4\text{H}^+/\text{TiO}^+$ ion ratio derived from depth profiles from one agglomerate, identified in a single cell of a Caco-2 cell exposed to $12.5 \mu\text{g}/\text{cm}^2$ of NM-104.

2.4.2 Toxicity

2.4.2.1 Cytotoxicity

Especially after repeated exposure, the presence of NPs interferes with the NRU assay and an increase of the absorbance values was observed when the concentration of NPs increased. To overcome the interference, the mean values were subtracted from the mean value of corresponding wells where no neutral red but only phosphate buffer solution was added at the end of the treatment.

No toxicity was observed with NM103 on differentiated Caco2 following an acute (24h or a long time (1 and 2 weeks) treatment followed or not by a recovery period (up to 1 week) (Figure 12).

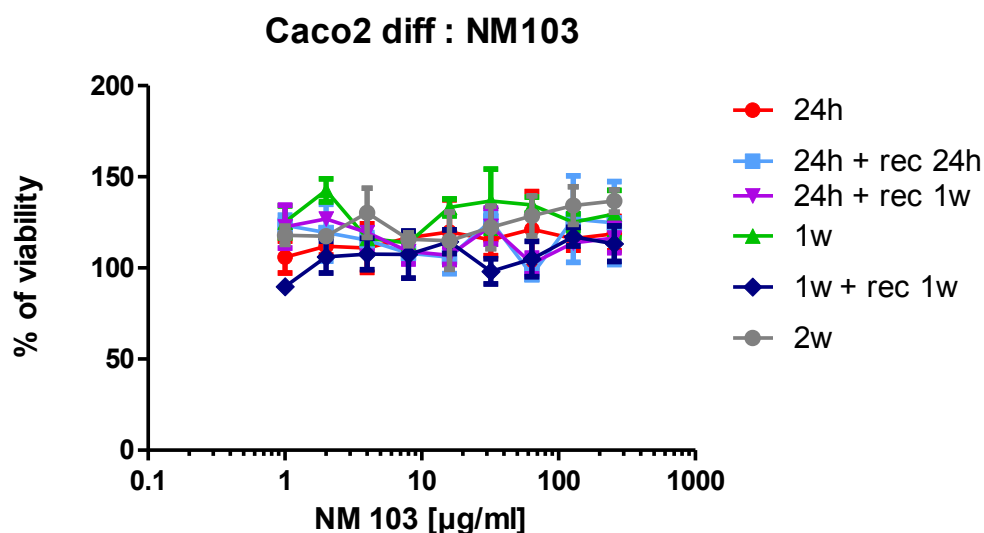


Figure 12: Cytotoxicity (Neutral Red Uptake) of NM103 on differentiated Caco2 after acute (24h) or repeated exposure (1 and 2 weeks) followed or not by a recovery period (up to 1 week)

Similarly, no cytotoxicity was noticed with NM104 on differentiated Caco2 following a similar treatment schedule (Figure 13).

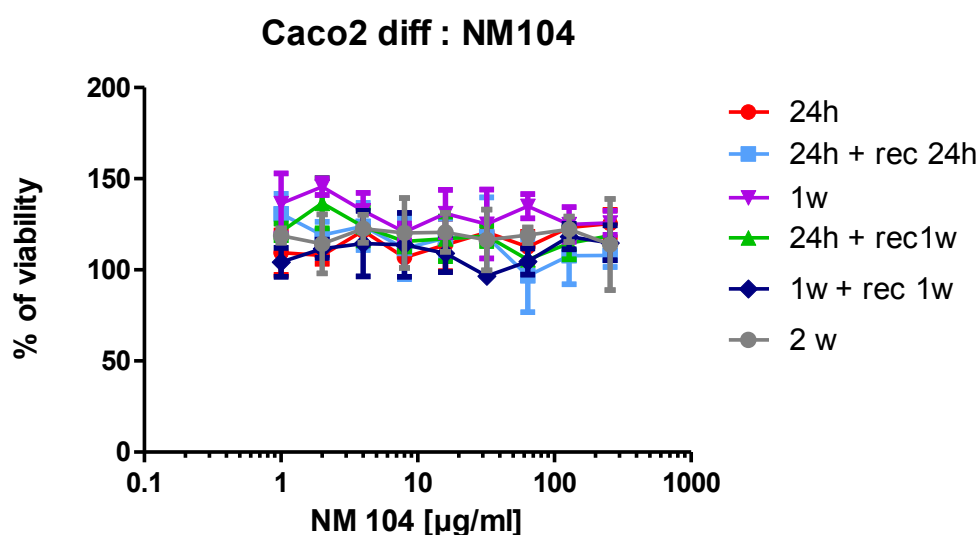


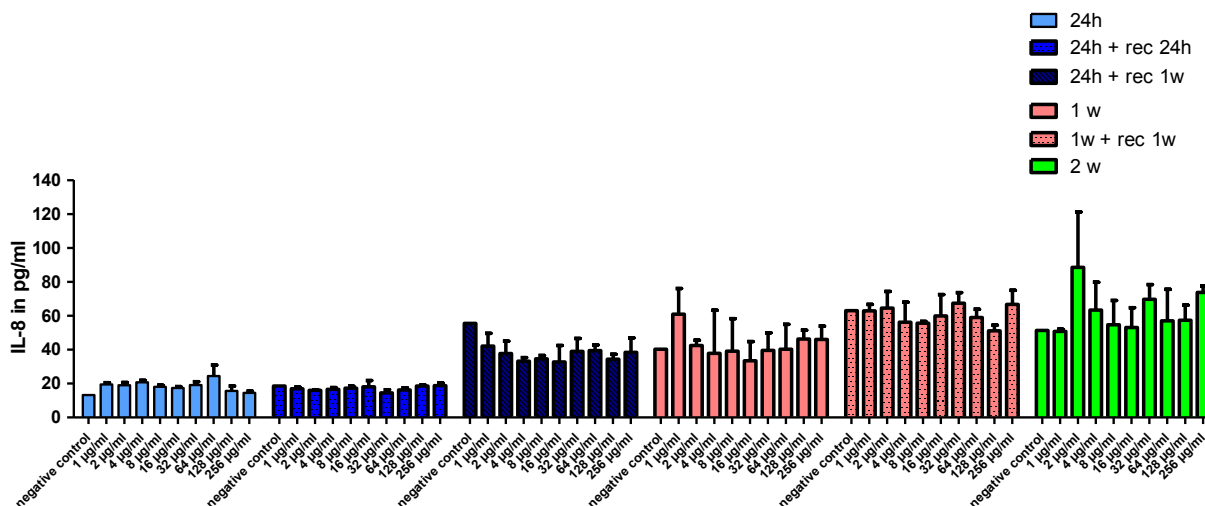
Figure 13: Cytotoxicity (Neutral Red Uptake) of NM104 on differentiated Caco2 after acute (24h) or long term (1 and 2 weeks) treatment followed or not by a recovery period (up to 1 week)

2.4.2.2 Interleukin 8 release

NM103 did not induce IL8 release on differentiated Caco2 following an acute (24h or a long time (1 and 2 weeks) treatment followed or not by a recovery period (up to 1 week) (Figure 14). Even if some increase can be observed punctually, no dose-response was noticed.

Similarly, no increase of IL8 release was noticed with NM104 on differentiated Caco2 following a similar treatment schedule (Figure 14B).

A



B

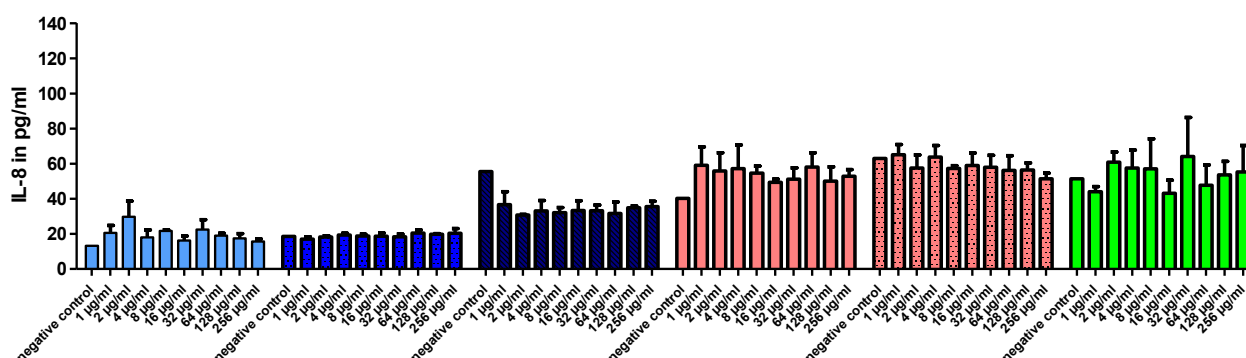


Figure 14: IL8 release (ELISA) from differentiated Caco2 cells after acute (24h) or long term (1 and 2 weeks) treatment with NM103 followed or not by a recovery period (up to 1 week): A) with NM103 and B) with NM104

2.4.2.3 Markers of toxicity by HCS

Simultaneously, 96 well plates were treated similarly to detect distinct effects using key markers: apoptosis (caspase 3), DNA breakage (phosphorylation of H2Ax) with High Content Screening (see WP5.6).

Unfortunately, due to the high level of NPs remaining on the cell cultures after repeated exposure, it was not possible to get accurate measurement using such a technique of immunolabelling.

2.4.2.4 Supplementary data: Genotoxicity

Aside the NANoREG project, the genotoxicity of NM103 and NM104 was tested *in vitro* on Caco2 cells for concentrations up to 256 µg/ml during a bilateral ANR/DFG project between France and Germany (SolNanoTox) with both, the comet assay modified with FpG enzyme for detection of oxidized bases and the micronucleus assay.

The outcomes are presented in table 1.

TEST	NM103	NM104
COMET ASSAY	Negative	Negative
COMET ASSAY +FpG	Negative	Negative
MICRONUCLEUS ASSAY	Negative*	Negative*

*due to the interference with the assay (NPs masking the cytoplasm and the potential presence of micronuclei) it cannot be concluded that no induction of micronuclei occurred at the highest concentrations tested.

Table 1: Response of differentiated Caco2 cells on exposure towards NM103 and 104 for 24h

2.5 Evaluation and conclusions

No difference was observed regarding the effects of NM103 and NM104 on differentiated Caco2 cells, neither for uptake nor for toxic effects. For both materials no genotoxicity was observed in Caco2 cells by application of the comet assay.

Although the intestinal Caco2 cells were shown to internalize both forms of TiO₂ easily, no toxicity was detected for the dose range tested. Even after a recovery period of one week, the nanoparticles were still observed in large amounts inside the cells, trapped into vesicles.

The absence of any change in IL8 release maybe due to the change of medium inclusive of nanoparticles every second or third day. This may have caused a reduction of inflammatory effects that would have been expected following repeated exposure.

High content screening is not recommended for studying the repeated *in vitro* exposure against TiO₂ as these particles alter the accuracy of the image analysis system. At the same time, these nanoparticles interfere with the micronucleus assay preventing any definite conclusion.

For all ToF-SIMS analysis no statistical analysis was performed, due to the fact that the experiments were intended to be a proof-of-principle investigation. The developed methodology showed for the first time that nanoparticle agglomerates could be counted and categorized in different size groups using ToF-SIMS from larger areas of interest. An exact statistical evaluation of the results would require, similarly to the statistical evaluation of nanoparticle aggregates with TEM, further experiments and the development of a statistical strategy to evaluate the acquired data within a new project framework.

2.6 Data management

Some of the presented experiments are based on techniques that have not yet been transferred into the laboratory routine. In particular, the establishment of an appropriate sample preparation of *in vitro* cultures has required longer than expected. Together with an unexpected set-back in personnel resources, this has resulted in the situation that no ISA-TAB-Nano template was established so far.

3 Deviations from the work plan

Due to unexpected illness of the major scientist responsible for ToF-SIMS investigations, the deliverable is completed with 4 months delay. It was expected to collect the *in vivo* samples from the oral genotoxicity experiment (sub task 4.5.4) which was planned to be performed on TiO₂. However, our plans changed for this sub-task as it was decided to move the activities on genotoxicity testing after oral exposure from ANSES on the sub task 4.5.5 coordinated by ISS with a 90-day study with silica. However as there is a high background

of silica in the environment, specific facilities are required which are only available in few laboratories such as ISS.

4 References / Selected sources of information (optional)

NANoREG [Guidance Document](#)

5 List of abbreviations (optional)

Not applicable

Annexes (optional)

Not applicable